



---

## Universe Model 10.0 overview

---

prepared by: Annie C. Robin, Céline Reylé, Frédéric Arenou,  
Carine Babusiaux, Artur Latorre i Musoll, Xavier  
Luri, Paola Sartoretti, Paolo Tanga, Eric Grux

approved by:

reference: GAIA-C2-TN-LAOB-AR-004-10

issue: 1

revision: 1

date: 2011-06-07

status: Issued

### **Abstract**

This Note describes the Universe Model as it is implemented in GaiaSimu 10.0.

## Document History

Issue	Revision	Date	Author	Comment
10	0	2011-06-07	AR	Version for cycle 10
9	0	2011-01-03	AR	Version for cycle 9
8	1	2010-05-11	AR	Version for cycle 8
7	2	2009-11-17	AR	Version used in cycle 7 and E2E test simulations completed
7	1	2009-10-16	AR	First version for cycle 7
6	1	2009-09-21	AR	Version used in cycle 6 simulations, final version
6	0	2009-09-21	AR	Version used in cycle 6 simulations, first draft

## Contents

<b>1</b>	<b>Introduction</b>	<b>5</b>
<b>2</b>	<b>Solar system objects</b>	<b>6</b>
<b>3</b>	<b>Stars in the Galaxy</b>	<b>8</b>
3.1	Galactic structure model inputs . . . . .	8
3.2	Pre-main sequence stars . . . . .	12
3.3	Rare objects . . . . .	12
3.3.1	Be stars . . . . .	13
3.3.2	Peculiar metallicity stars . . . . .	13
3.3.3	Wolf Rayet stars . . . . .	13
3.4	Implementation for simulations in GaiaSimu and tests . . . . .	13
<b>4</b>	<b>Simulation of binary and multiple objects</b>	<b>14</b>
<b>5</b>	<b>Variability</b>	<b>16</b>

5.1	Regular and semi-regular variables . . . . .	16
5.2	Cataclysmic variable stars . . . . .	16
5.3	Microlensing events . . . . .	17
5.4	M-dwarfs flare . . . . .	17
5.5	R Coronae Borealis and DY Persei stars . . . . .	18
5.6	Eclipsing binaries . . . . .	18
5.7	Extragalactic variabilities . . . . .	18
5.8	Gamma ray Burst . . . . .	19
<b>6</b>	<b>Planetary nebulae</b>	<b>19</b>
<b>7</b>	<b>Exoplanet simulation</b>	<b>20</b>
<b>8</b>	<b>Extinction model</b>	<b>20</b>
<b>9</b>	<b>Extragalactic objects</b>	<b>21</b>
9.1	Resolved galaxies . . . . .	21
9.2	Unresolved galaxies . . . . .	22
9.3	Quasars . . . . .	22
9.4	Supernovae . . . . .	24
<b>10</b>	<b>Backgrounds</b>	<b>25</b>
<b>11</b>	<b>Radiation environment</b>	<b>25</b>
<b>12</b>	<b>Spectral libraries</b>	<b>25</b>

**13 References****29**

# 1 Introduction

The Universe Model developed for the simulation of the mission is a set of algorithms for computing the positions at any time, and observational properties of any objects expected to be observed by the Gaia instruments.

The distributions of these objects and the statistics of observables should be as realistic as possible for simulations to be usable for estimating telemetry, testing software, simulating images, etc. The algorithms have to be optimised in order that the simulations can be performed in reasonable time and can be redone when necessary. The complexity of the model is expected to increase during the preparation of Gaia.

Objects which will be, in fine, simulated are: solar system objects (planets, satellites, asteroids, comets), Galactic objects (stars, nebulae, stellar clusters, diffuse light), extragalactic objects (galaxies resolved in stars, unresolved but extended galaxies, quasars and active galactic nuclei, supernovae). For each of these simulated objects one needs to have their full 3D spatial distribution together with their spectral characteristics (to be able to compute photometry and spectroscopy, stable or variable in time), and their motions (for astrometric computations and for spectral corrections). Gravitational lensing for stars and galaxies are also to be simulated.

Here we describe the universe model as it is available in version 10 of GaiaSimu.

In order to simulate the sky content, the sky is subdivided in smaller regions with a Hierarchical Triangular Mesh (HTM, see <http://skyserver.org/htm/>). The source generation uses a consistent random number generator on sky regions so that exactly the same list of sources is always obtained in a given HTM, if no input parameters have been changed. Each source possesses a unique identifier based on this HTM number, the full input and output format of the identifier being described in Arenou et al. (2008).

The Universe Model package consists in several separate packages: a package containing the classes for generating the sources (called *generator*) and a package for computing source characteristics (called *source*). The spectral libraries are put in a different package (*speclibrary*) and the variability classes and methods in another one (*variability*).

In each region of sky *AstroSources* are created using the class *AstroSource*. It is in charge of modelling an observable source and its parameters. It contains the *PhysicalParameters*, the *Astrometry*, the *Shape*, the *Photometry* and the *Spectroscopy* classes (figure 1). Note that the source generation method does not initialize the sources *Spectroscopy* attribute and it does not use the appropriate spectrum in the *Photometry*; the spectra should be found in the *SpectralLibraries* and should be set after the source generation process.

The relativistic corrections for all types of objects (including aberration and light bending by the Solar System main bodies) now use the *FullGaiaRelativityModel* included in GaiaTools.

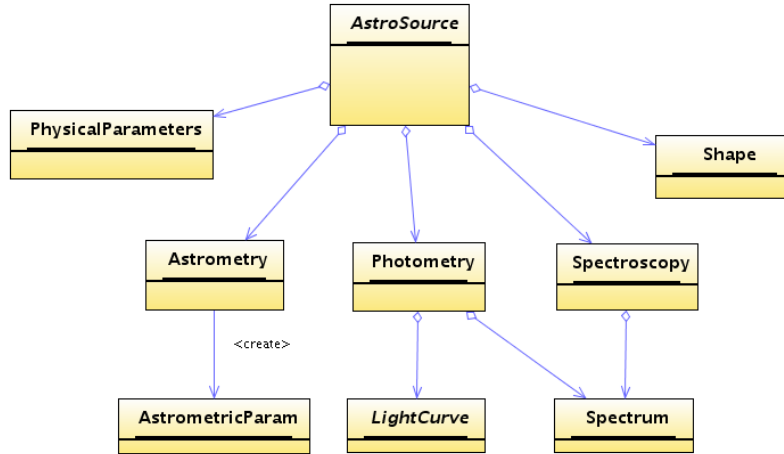


FIGURE 1: Main classes describing an AstroSource.

Another previously used model (SimpleGaiaRelativityModel, also available in GaiaTools) has been kept internally available in the `gaiasimu.universe.Relativity` class just in case some back-compatibility is needed, but it is not actually used in the simulations and will be completely removed in cycle 11.

In the following we describe the generation of the different type of objects and the computation of their relevant characteristics, as they are implemented in the simulations, and the planned improvements for next cycles.

## 2 Solar system objects

Solar system objects model include both real objects with ephemerides (sun, moon, planets and their satellites, minor planets and known big asteroids, known periodic comets) and simulated objects (smaller asteroids, new comets, Kuiper belt objects and centaurs).

The Solar System objects (SSOs) are only a little sample of the total number of objects expected to be observed by Gaia, but their peculiarities strongly condition the design of this part of the Universe Model. The semi-empirical statistical approach (constrained by observations) considered in the other parts of the Universe Model is no longer valid (in this first version of the Solar System Module) due to the high apparent motions of the SSOs. The reason is quite simple: it is not possible to generate a catalogue of objects (along with their physical information) for a certain (static) sky region, since the observed objects in that direction depends on time. Therefore, to generate a catalogue of SSOs we would need to specify both the sky region and observation time. However, if the simulations are required to be done in a reasonable computational time, the computation of the ephemerides along the mission of a set of ( $\sim 10^5$ ) SSOs is not feasible

in this first approach.

To solve this problem, the simulation must not be based on a reliable statistical model, but on catalogues containing orbital elements of SSOs, stored on disk. By computing SSOs ephemerides in time, and crossing the obtained positions with the Gaia Scanning Law, only the transiting ones (i.e. the SSOs inside one of the FoVs) at any time along the mission are selected. This transits list contains all the candidates expected to be observed, and obviously, it contains also the transit time in the corresponding FoV, the astrometric data and the apparent magnitude of these objects. This is the basic input for the simulation of the Solar System.

We must note several things. Firstly, the input transits list must be only computed once, and this strategy avoids to compute the position of all the sources for each time step inside the simulation to obtain the candidates to be detected. This is a large computational advantage. Secondly, we do not need to specify a sky region to run a simulation, but a time interval instead. We have to recall that this strategy does not make this part of the Universe Module totally independent of the Instrument Model, which is an inconvenient. However, and finally, the previous step of computing the transits list makes the initialization of the Solar System Module to be much faster than if we considered, as a starting point, some statistical model of spatial distribution of the different types of SSOs (and how their positions propagate with time).

The transits list is provided by F. Mignard after a computation using a set of osculating elements available from several sources (see GAIA\_FM\_019 for details). Some other information about these objects is available in a catalogue compiled by P. Tanga and F. Mignard. The current simulations use a set of minor bodies selected following specific needs (including MBOs, NEOs, Trojans and KBOs), but do not consider multiplicity features, shape complexity nor surface brightness. These data are used by the generator to initialize the Solar System Module (sources), and to provide a list of candidates in a user-defined time interval inside the mission. This output has just been used to generate some test GASS simulations, which have been processed by IDT for producing the data needed to test the SSO pipeline. After some validations some inconsistencies in astrometry at the level of a few arcsec have been found. The problem is being investigated but currently unsolved.

In the same way, some other tests, basically concerning astrometry checks, have been performed to guarantee the overall consistency. This is, in fact, the most delicate point: since the computations are not done from the beginning to the end inside GaiaSimu, some discrepancies can easily arise. For instance, the implementation of the Gaia scanning law in the transits computations must be consistent with GaiaSimu; if this consistency it is not achieved, the output of the Solar System Module will not match with the detection predictions of GASS (for instance), and, therefore, realistic telemetry will not be obtained.

The tests have been useful to show some structural problems: the design of the Universe Model is not optimal for our Solar System needs. For example, correct calls to the Klioner routines (the relativity corrections for SSOs are not the same than for stars), and some changes in the

internal usage of the class *Astrometry* have been implemented in order to obtain correct results. However, a future redesign of the astrometry computations is needed in order to make more transparent the usage of the Solar System Module. Moreover, the implementation of SSOs must also grow in complexity in the future in several aspects. For example, a star-like motion is considered for SSOs around the transit detection. It has been considered sufficient to implement a linear motion of the asteroid in the focal plane since SSOs spends about 30 sec to cross a FoV, but more high-precision recomputations (but only close to the detection) can be performed solving the Kepler equation with the osculating elements of the objects (specially high-speed objects, where second-order effects can be important).

Complex asteroid shapes are available. All asteroids are considered to be uniformly illuminated disks, but a sub-sample of them (100) have complex shape models, allowing the user to simulate the effect of irregular shapes, illumination, phase defect on the astrometry of the asteroid. Multiple systems are to be implemented in the future.

## 3 Stars in the Galaxy

Gaia will detect and measure about 1 to 1.5 billion objects that are part of the Galaxy, providing the main contribution to the object database. A reliable model of the stellar distribution over the sky up to magnitude 20-21 is most important, with reliable spectral distribution and motions for these objects. The current version of a Galaxy model has been implemented in java, based on the Besançon Galaxy Model (Robin et al. (2003), here after BGM), and the 3D extinction model from Drimmel (2002).

### 3.1 Galactic structure model inputs

Here we recall the main ingredients on which the star simulations are based.

The stellar population synthesis model of the Galaxy constructed in Besançon is able to simulate the stellar content of the Galaxy by modelling four distinct stellar populations: the thin disc, the thick disc, the outer bulge and the spheroid. It can be used to generate stellar catalogues for any given direction, and returns information on each star such as magnitude, colour, and distance as well as kinematics and other stellar parameters.

The approach of the Galactic model is semi-empirical as it is based on theoretical considerations (stellar evolution, Galactic evolution and Galactic dynamics) but is constrained by observations (the local luminosity function, the age-velocity dispersion relation, the age-metallicity relation). The Galactic potential is calculated in order to self-consistently constrain the disc scale height, the thin disc being subdivided into 7 isothermal components of ages varying from 0-0.15 Gyr for the youngest to 7-10 Gyr for the oldest. For computing the scale height at the solar position as a function of age (Bienayme et al. 1987a,b), the Boltzmann equation (first moment at the



TABLE 2: Age, metallicity ([Fe/H] (mean and dispersion about the mean), radial metallicity gradient (dex/kpc), initial mass function (IMF), and star formation rate (SFR) of the stellar components.

	Age (Gyr)	[Fe/H] (dex)	$\frac{d[Fe/H]}{dR}$	IMF	SFR
Disc	0-0.15	$0.01 \pm 0.12$	-0.07	$dn/dm \propto m^{-\alpha}$ $\alpha = 1.6$ for $m < 1M_{\odot}$ $\alpha = 3.0$ for $m > 1M_{\odot}$	constant
	0.15-1	$0.03 \pm 0.12$			
	1-2	$0.03 \pm 0.10$			
	2-3	$0.01 \pm 0.11$			
	3-5	$-0.07 \pm 0.18$			
	5-7	$-0.14 \pm 0.17$			
	7-10	$-0.37 \pm 0.20$			
Thick disc	11	$-0.78 \pm 0.30$	0.00	$dn/dm \propto m^{-0.5}$	one burst
Stellar halo	14	$-1.78 \pm 0.50$	0.00	$dn/dm \propto m^{-0.5}$	one burst
Bulge	10	$0.00 \pm 0.40$	0.00	$dn/dm \propto m^{-2.35}$ for $m > 0.7M_{\odot}$	one burst

first order with the plane parallel approximation) is used assuming an age-velocity dispersion relation deduced from Hipparcos observations (Gomez et al. 1997).

The distribution in the Hess diagram split into several age bins is obtained from an evolutionary model which starts with a mass of gas, generates stars of different masses assuming an Initial Mass Function and a star formation rate history, and makes these stars evolve along evolutionary tracks. The evolution model is described in Haywood et al. (1997a,b). The evolutionary model produces a file describing the distribution of stars per element volume in the space ( $M_V$ ,  $T_{\text{eff}}$ , Age). Similar Hess diagrams are also produced for the bulge, the thick disc and the spheroid populations, assuming a single burst of star formation and ages of 10 Gyr, 11 Gyr and 14 Gyr respectively.

Since cycle 6, the stellar luminosity function is the one for primary stars (single stars, or primary stars in multiple systems). This is done by adjusting the multi-slope IMF over the luminosity function of primaries in the solar neighbourhood from Reid et al. (2002). This ensures that, when generating the secondaries, the total number of stars and their distribution in mass is still compatible with the statistics in the solar neighbourhood. This IMF goes down to the hydrogen burning limit, and include disc stars down to  $M_V=24$ . It corresponds to spectral types down to about L5.

A summary of age and metallicities, star formation history and initial mass function for each population is given in table 1.

In order to compute the  $N$  number of stars at any point in the Galaxy of a given population we make use of the equation of stellar statistics :

$$N = \int_0^{R_{\text{max}}} \rho(R, \theta, z) \times \Phi(M_V, T_{\text{eff}}, \text{Age}) \omega r^2 dr$$

where  $\rho$  is the density law of the population,  $r$  the distance to the sun,  $(R, \theta, z)$  the galactocentric cylindrical coordinates,  $\omega$  the solid angle,  $N$  is the theoretical number of stars in a volume element with the intrinsic parameters  $M_V$ ,  $T_{\text{eff}}$ , and Age. In order to simulate catalogues, from this number a random drawing is performed to produce an integer number of stars, which follows a Poisson distribution of expectation (and variance)  $N$ .

The density law of each population has been described in Robin et al. (2003). However the disc and bulge density has been slightly changed since then. Revised density laws are given in table 2. In this table for simplicity the density formulae do not include the warp and flare, which are added as a modification of the position and thickness of the mid-plane.

The flare is the increase of the thickness of the disc with galactocentric distances :

$$k_{\text{flare}} = 1. + g_{\text{flare}} \times (R - R_{\text{flare}})$$

with  $g_{\text{flare}} = 0.545 \times 10^{-6} \text{ pc}^{-1}$  and  $R_{\text{flare}} = 9500 \text{ pc}$ .

The warp is modelled as a symmetrical S-shape warp with a linear slope of 0.09 starting at galactocentric distance of 8400 pc Reyl  et al. (2009). Moreover a spiral structure has been added with 2 arms, as determined in a preliminary study by De Amores & Robin (in prep.). The parameters of the arms are given in table 3.1.

For cycle 10, the thick disc scale height, scale length and normalisation have been changed to allow more reliable simulations at low latitudes (Robin et al, in prep.)

Metallicity  $[\text{Fe}/\text{H}]$  is computed through an empirical age-metallicity relation from Twarog (1980). For each age and population component the metallicity is drawn from a gaussian, with a mean and a dispersion, as given in table 1. One also accounts for radial metallicity gradient for the thin disc,  $-0.7 \text{ dex/kpc}$ , but no vertical metallicity gradient. Alpha elements are computed as a function of the population and the metallicity. For the bulge, thick disc and halo, the abundance in alpha element is drawn from a random around a mean value which depends on  $[\text{Fe}/\text{H}]$ . Formulae are given in table 3.1. For the thin disc, the formula is a fit to the mean location of thin disc stars from Bensby et al. (2010) study. For the thick disc and the bulge the formulae are from Gonzalez et al. (2011).

Kinematics is computed assuming a velocity ellipsoid for each age and population component. The characteristics of these ellipsoids are given in table 4. The asymmetric drift for the thin disc is computed following the relation:

$$V_{\text{ad}} = \frac{\sigma_U^2}{2V_{\text{LSR}}} \left\{ \frac{R}{\rho} \frac{d\rho}{dR} + 2 \times \frac{R}{\sigma_U} \frac{d\sigma_U}{dR} + \left(1 - \frac{\sigma_V^2}{\sigma_U^2}\right) + \left(1 - \frac{\sigma_W^2}{\sigma_U^2}\right) \right\}$$

where  $\frac{d\rho}{dR}$  is the density gradient.  $V_{\text{LSR}} = 226 \text{ km s}^{-1}$  is obtained, as well as the whole rotation

TABLE 3: Density laws and associated parameter of the stellar components.  $a^2 = R^2 + \frac{z^2}{\epsilon^2}$  where  $R$  is the galactocentric distance,  $z$  is the height above the Galactic plane, and  $\epsilon$  is the axis ratio. Values of  $\epsilon$  are given in table 2 of Robin et al. (Robin et al. 2003). For simplicity the disc density law is given here without the warp and flare (see text for their characteristics).  $d_0$  are normalization constants. For the bulge,  $x, y$  and  $z$  are in the bulge reference frame and values of  $N, x_0, y_0, z_0$  and  $R_c$  as well as angles from the main axis to the Galaxy reference frame are given in Robin et al. (2003), table 5.

	density law	
Disc	$\rho_0/d_0/k_{flare} \times \{\exp(-(a/h_{R+})^2) - \exp(-(a/h_{R-})^2)\}$ with $h_{R+} = 5000$ pc, $h_{R-} = 3000$ pc $\rho_0/d_0 \times \{\exp(-(0.25 + a^2/h_{R+}^2)^{1/2}) - \exp(-(0.25 + a^2/h_{R-}^2)^{1/2})\}$ with $h_{R+} = 2530$ pc, $h_{R-} = 1320$ pc	if age $\leq 0.15$ Gyr if age $> 0.15$ Gyr
Thick disc	$\rho_0/d_0/k_{flare} \times \exp(-\frac{R-R_\odot}{h_R}) \times (1 - \frac{1/h_z}{x_l \times (2+x_l/h_z)} \times z^2)$ $\rho_0 \times \exp(-\frac{R-R_\odot}{h_R}) \times \frac{\exp(x_l/h_z)}{1+x_l/2h_z} \exp(-\frac{ z }{h_z})$ with $h_R = 4000$ pc, $h_z = 1200$ pc	if $ z  \leq x_l, x_l=72$ pc if $ z  > x_l$
Spheroid	$\rho_0/d_0 \times (\frac{a_c}{R_\odot})^{-2.44}$ $\rho_0 \times (\frac{a}{R_\odot})^{-2.44}$	if $a \leq a_c, a_c = 500$ pc if $a > a_c$
Bulge	$N \times \exp(-0.5 \times r_s^2)$ $N \times \exp(-0.5 \times r_s^2) \times \exp(-0.5(\frac{\sqrt{x^2+y^2}-R_c}{0.5})^2)$ with $r_s^2 = \sqrt{[(\frac{x}{x_0})^2 + (\frac{y}{y_0})^2]^2 + (\frac{z}{z_0})^4}$	$\sqrt{x^2+y^2} < R_c$ $\sqrt{x^2+y^2} > R_c$

TABLE 4: Provisional parameters of the 2 arms of the spiral structure.

Parameter	1st arm	2nd arm
Internal radius in kpc	3.426	3.426
Pitch angle in radian	4.027	3.426
Phase angle of start in radian	0.188	2.677
Amplitude	1.823	2.013
Thickness in the plane	4.804	4.964

TABLE 5: Abundances in iron and  $\alpha$  elements used in the simulations for each stellar population.

Population	$< [\text{Fe}/\text{H}] >$	$\sigma$	$\frac{d[\text{Fe}/\text{H}]}{dR}$	$< [\alpha/\text{Fe}] >$	$\sigma$
Disc	+0.03 to -0.37	0.10 to 0.20	-0.07	-0.03-0.24 $\times$ [Fe/H]	0.1
Thick disc	-0.78	0.30	0.00	0.392-exp(1.19375 $\times$ [Fe/H]-1.3038)	0.2
Stellar halo	-1.78	0.50	0.00	0.4	0.2
Bulge	0.00	0.40	0.00	0-0.334 $\times$ [Fe/H]+0.134	0.2

TABLE 6: Velocity dispersions ( $\sigma_U, \sigma_V, \sigma_W$ ), asymmetric drift  $V_{\text{ad}}$  at the solar position and velocity dispersion gradient  $\frac{d \ln(\sigma_U^2)}{dR}$ , where  $\sigma_U$  is expressed in  $\text{km s}^{-1}$  and  $R$  in kpc.

	Age (Gyr)	$\sigma_U$ ( $\text{km s}^{-1}$ )	$\sigma_V$ ( $\text{km s}^{-1}$ )	$\sigma_W$ ( $\text{km s}^{-1}$ )	$V_{\text{ad}}$ ( $\text{km s}^{-1}$ )	$\frac{d \ln(\sigma_U^2)}{dR}$
Disc	0-0.15	16.7	10.8	6	3.5	-0.2
	0.15-1	19.8	12.8	8	3.1	
	1-2	27.2	17.6	10	5.8	
	2-3	30.2	19.5	13.2	7.3	
	3-5	36.7	23.7	15.8	10.8	
	5-7	43.1	27.8	17.4	14.8	
	7-10	43.1	27.8	17.5	14.8	
Thick disc		67	51	42	53	0
Spheroid		131	106	85	226	0
Bulge		113	115	100	79	0

curve, after fitting the Galaxy mass model to the observed rotation curve (Robin et al. 2003).

In the framework of the Gaia simulator, only the distribution of the stars, their intrinsic parameters and their motions are obtained from the BGM. Transformations to apparent magnitude, colours and spectra for the Gaia instruments are done using the Gaia spectral library and the Gaia instrument model.

Most parameters, like the solar motion in the LSR are taken from the parameter data base. However the BGM uses specific values for the position of the Sun relative to the Galactic center (8.5 kpc from the sun and 15 pc from the plane) rather than the values of the database, because they are the values used to validate the BGM with star counts up to now.

## 3.2 Pre-main sequence stars

From cycle 9, pre-main sequence stars are generated using evolutionary tracks from Valls-Gabaud, Pichon, et al (in prep.). They have been produced using the code of stellar evolution CESAM for masses between 0.7 and 3. solar masses. The volume density along the tracks have been computed consistently with a constant star formation rate.

## 3.3 Rare objects

For the needs of the simulator, some rare objects have been added to the BGM Hess diagram.

### 3.3.1 Be stars

Be stars are simulated as a proportion of 29% of O7-B4 stars, 20% of B5-B7 stars and 3% of B8-B9 stars (Jaschek et al. 1988; Zorec & Briot 1997). They are attributed a parameter linked with the line strength in order to attribute them a spectrum from the spectral library (see sect.12). This parameter is the ratio between the envelope radius and the stellar radius ( $R_{env}/R_{star}$ ). In order to simulate the variation of the emission lines with time this parameter is set randomly between 1.2 and 6.9 at any time.

### 3.3.2 Peculiar metallicity stars

Two types of peculiar metallicity stars are simulated, following Kurtz (1982); Kochukhov (2007); Stift & Alecian (2009).

- Am: 12% of A stars on the main sequence in the  $T_{eff}$  range 7400 K - 10200 K are set to be Am stars. 70% of these Am stars belong to a binary system with period from 2.5 to 100 days. They are forced to be slow rotators : 67% have  $v \sin i < 50$  km/s and 23% have  $50 < v \sin i < 100$  km/s.
- Ap/Bp: 8% of A and B stars on the main sequence in the  $T_{eff}$  range 8000 K - 15000 K are set to be Ap or Bp stars. They are forced to have a smaller rotation :  $v \sin i < 120$  km/s.

### 3.3.3 Wolf Rayet stars

Wolf Rayet (WR) densities are computed following the observed statistics from the VIIth catalogue of Galactic Wolf-Rayet stars of van der Hucht van der Hucht (2001). The local column density of WR stars is  $2.9 \times 10^{-6} \text{ pc}^{-2}$  or volume density  $2.37 \times 10^{-8} \text{ pc}^{-3}$ . Among them 50% are WN, 46% are WC and 3.6% are WO. The absolute magnitude, colours, effective temperature, gravity and mass have been estimated from the literature. The masses and effective temperature vary considerably from one author to another. As a conservative value, we assume that the WR stars have masses of  $10 M_{\odot}$  in the mean, an absolute V magnitude of -4, a gravity of -0.5, and an effective temperature of 50,000K.

## 3.4 Implementation for simulations in GaiaSimu and tests

The Universe model is used by GaiaSimu in two ways : stars can be created one by one, with desired characteristics, or star counts can be computed all at ones in order to estimate the telemetry in given fields. Both ways have been tested to give similar results within the expected Poisson noise generated in the star by star method.

Several tests have been performed in order to ensure the reliability of model predictions. First, a detailed comparison of predicted star counts in the G band has been done between the Fortran version (original code) and the java version (Gaia simulator implementation) to ensure the reliability of the new coding. Second, the star counts have been compared with GSC-II star counts transformed into the G band over all sky (Drimmel et al. 2003). From this comparison the reliability of the predicted counts is assessed to be at the level of 15% at medium and high Galactic latitudes at magnitude  $G=17$ . In the Galactic plane uncertainties are larger due to the incomplete knowledge of the extinction distribution and the fact that photographic surveys suffer from high crowding at faint magnitudes. Similar tests have also been used to compare with star counts in the near infrared at low latitudes on which the impact of assumptions on the extinction is lower. However the reliability of the counts at small scale are still uncertain at a level of 50% in the Galactic central regions, but at larger scale (degree) the counts can be considered reliable enough for estimating the telemetry. In the future we shall consider to increase the reliability of the counts in the Galactic plane by improving the Galactic structure model and the extinction model.

## 4 Simulation of binary and multiple objects

Binary and multiple objects are considered for solar system objects and for stars. For the moment, nothing is planned for simulating groups of galaxies, except the local group (see below).

The BGM model produces only single stars. Simulations of binaries have been introduced in the Gaia simulator in the following way, see DMS-FA-03 (GAIA-C4-TN-OPM-FA-008-3) then GAIA-C2-TN-OPM-CB-006, and Arenou (2010).

In a first step (in 2003), solar-type star-like binaries were introduced only. Then simulations based on Soderhjelm proposal (DMS-SS-05, 2004) were implemented. For each single star, a companion was created (or not) with some probability depending on the spectral type of the primary. The distribution of secondaries in separation and mass ratio was taken, the system could be visual, or astrometric binary with a main sequence or white dwarf companion. For visual systems, the initial luminosity was shared between components and the mass ratio followed from the magnitude difference, otherwise it was based on the luminosity of the primary.

Unfortunately, the simulations were not satisfactory for several reasons: the single star fraction was severely underestimated towards low mass stars, multiple stars were not handled, and the resulting luminosity function was not fully consistent with the mass distribution. The generation of the secondaries has completely changed at cycle 6, thanks to the new possibility of selecting on the HR diagram a companion of a given mass, with the same age as the primary. At the same time the single stars and primaries were chosen so as to follow the luminosity function (LF) of primaries in the solar neighbourhood (see above), not the LF of unresolved binaries. This rendered possible to accomplish the simulation the following way, trying to be consistent with

the known observable properties.

With some probability, the binarity proportion having been reevaluated as a function of the type (mass) of the primary, an (initially single) star given as input can give birth to a system. This system has the given star as primary, and a secondary which mass ratio is chosen at random, depending in a not-so-simple manner (it was taken for the available statistics) from the spectral type of the primary and on the binary period. As indicated above, the mass and age of secondary allow it to obtain physical parameters computed using the Hess diagram distribution in the Besancon model; with some probability this secondary can also be a white dwarf. Depending on the primary mass, the separation between components is chosen, and the period follows from Kepler third law. Drawing the random eccentricity has also been refined, as it now depends on the primary type and period of the system. The other orbital parameters are chosen at random. At cycle 6, ternary systems have been reintroduced, possibly trapezium, and quinary systems are available from cycle 8 on.

A large effort has been put at trying to ensure that simulated multiple stars numbers are in accordance with latest fractions known from available observations, and this is daily tested by JUnit tests. This does not apply to main sequence stars only, attention being paid to white dwarfs and giant stars in systems too. For instance, thanks to new (single) white dwarf mass distributions, the observational numbers of white dwarf components are now well reproduced from cycle 7 on, with few ad-hoc adaptations.

Multiple star simulations are of course not static. Beyond the Galactic properties of multiple stars, the astrometric, spectroscopic (radial velocity) and photometric (eclipses) effects of these objects have to be taken into account: in the course of the simulations of Gaia transits, the orbits are thus computed, the positions of both components are modified, and the astrometry and photometry of the system is modified accordingly.

In particular, this means that the eclipses have to be computed, whatever the state of the system. This has been done at cycle 7, interfacing the software code developed by CU4 DU436, as it represented several man-years obviously impossible to allocate otherwise in CU2. Besides, it should now be noted that the DU436 code is used not only for eclipsing binaries, but also to reject (possible non eclipsing) unrealistic short period systems. Still, although most has been already implemented, several kind of contact binaries (e.g. common envelope W UMa) should be improved for what concerns the flux normalisation, as is the case for exoplanet transits.



## 5 Variability

### 5.1 Regular and semi-regular variables

The present version of the UM implements six types of regular and semi-regular stellar variability: Cepheid, RRab, RRC,  $\delta$  Scuti, roAp, ACV, Semi-regular. The variability probabilities depend on the position in the HR diagram. A summary of the variable type characteristics is given in table 5.1. Period and amplitude are taken randomly from a 2D distribution defined for each variability type (Eyer et al. 2005). For Miras, we also consider the following period/luminosity relation:  $P = (-M_{Bol} + 2.06)/2.54$  (Feast et al. 1989, MNRAS 241, 375).

The period/luminosity relation for Cepheids is not implemented yet.

The different light curves modelled depending on the variability type are described in Reyl   et al. (2007). For RRab, different light curve templates are used. They are simulated using the package LCmodel.jar produced by CU7. Light curves for GammaDor et ZCCeti are also computed with this package.

The variation of the radius and radial velocity are computed accordingly to the light variation, for stars with radial pulsations (RRab, RRC, Cepheids,  $\delta$  Scuti, SemiRegular, and Miras).

A unique seed is used for the generation in order to ensure that at each simulation the same stars are found to be variable with the same characteristics. No colour effect is introduced yet but it could be included if necessary.

The light curve of the regular or semi-regular variable stars is defined as follows, with  $\omega t = 2\pi \frac{t}{P} + \phi$  ( $P$  is the period,  $\phi$  is the phase) :

Variability type	Light curve
Cepheid	$S = 0.418 \sin(\omega t - 20.76) + 0.1419 \sin(2\omega t - 63.76) + 0.0664 \sin(3\omega t - 91.57) + 0.0354 \sin(4\omega t - 112.62) + 0.020 \sin(5\omega t - 129.47)$
$\delta$ Scuti, roAp, RRC, Miras	$S = 0.5 \sin(\omega t)$
ACV	$S = -0.5 \cos(2\omega t)(1 - f * \cos(\omega t))/(1 + f/2)$ , $f$ random from 0 to 1
SemiRegular	Inverse Fourier Transform of a gaussian in frequency space

### 5.2 Cataclysmic variable stars

Dwarf novae and Classical novae are cataclysmic variable stars consisting of close binary star systems in which one of the components is a white dwarf. We simulated half of the white dwarfs in close binary systems with period  $< 14$  hours as dwarf novae. The light curve is simulated by a linear increase followed by an exponential decrease. The time between two bursts, the



TABLE 7: Characteristics of the regular and semi-regular variable types. Localization in the (spectral type, luminosity class) diagram, probability P in this region, stellar population and metallicity range which are concerned.

Type name	Spec. type	Lum. C.	P	Pop.	[Fe/H]	Mbol	Teff
$\delta$ Scuti (a)	A0:F2	III	0.3	all	all	—	—
$\delta$ Scuti (b)	A1:F3	IV:V	0.3	all	all	—	—
ACV (a)	B5:B9	V	0.016	thin disc	-1 to 1	—	—
ACV (b)	A1:A8	IV:V	0.01	thin disc	-1 to 1	—	—
Cepheid	F5:G0	I:III	0.3	thin disc	-1 to 1	—	—
RRab	A8:F5	III	0.4	spheroid	-4 to -1	—	—
RRc	A8:F5	III	0.1	spheroid	-4 to -1	—	—
RoAp	A0:A9	V	0.001	thin disc	-1 to 1	—	—
SemiReg (a)	K5:K9	III	0.5	all	all	—	—
SemiReg (b)	M0:M9	III	0.9	all	all	—	—
Miras	M0:M9	I:III	1.	all	all	-4.5:-3	2500:3500
ZZCeti	White dwarf	—	1	all	all	—	10800:12300
GammaDor	F0:F5	V	0.3	all	all	—	—

amplitude, the rising time and the decay time are drawn from gaussian distributions derived from OGLE observations (Wyrzykowski & Skowron, private communication).

The other half of white dwarfs in such systems is simulated as a Classical novae. Their light curve are computed from the package LCmodel.jar produced by CU7.

### 5.3 Microlensing events

Microlensing effects are generated assuming a map of event rate as a function of Galactic coordinates (l,b). The probabilities of lensing over the sky are drawn from the study of Han (2008).

The Einstein crossing time is also a function of the direction of observation in the bulge, obtained from the same paper. The Einstein time of the simulated events are drawn from a gaussian distribution centered on the mean Einstein time. The impact parameter follows a flat distribution from 0 to 1. The time of maximum is uniformly distributed and completely random, from the beginning to the end of the mission. The Paczynski formula is used to compute the light curve.

### 5.4 M-dwarfs flare

The statistics for M-dwarf flares are mainly based on Kowalski et al. (2009) and their study on SDSS data: 0.1% of M0-M1 dwarfs, 0.6% of M2-M3 dwarfs, and 5.6% of M4-M6 dwarfs are

flaring. Light curve is described as follows:

$$f = 1 + \exp(-(t - t_0)/\tau) \text{ for } t > t_0; f = 1 \text{ for } t < t_0$$

$$mag = mag_0 - 1.32877 \times A \times 2.5 \times \log_{10}(f)$$

where  $t_0$  is the time of the maximum,  $\tau$  is the decay time (in days, random between 1 and 15 minutes),  $mag_0$  is the baseline magnitude of the source star,  $A$  is the amplitude in magnitudes (drawn from a gaussian gaussian distribution with  $\sigma = 1$  and  $x_0 = 1.2$ ).

## 5.5 R Coronae Borealis and DY Persei stars

RCrB are carbon stars, however the link with the carbon stars is not fully understood and confirmed. If we assume the distribution of RCrB and DY Per stars follows this of Carbon stars, we can estimate a rate of “outbursting” carbon stars based on the LMC studies. There are around 8000 Carbon stars known in the LMC (e.g. Kontizas et al. (2001)). Soszyński et al. (2009) based on the OGLE data set the number of candidates for the RCrBs to 23. They also discovered a large number of potential DY Persei stars (around 600). This gives us the rates of 0.003 and 0.075 of Carbon stars exhibiting RCrB and DYPer behaviour, respectively.

Apart from their main feature - the dip - they exhibit some small amplitude irregular variability, which can be approximated with two periods:

$$m_b(t) = mag_0 + \sum_{i=0}^2 \frac{1}{2} a_i \cos 2\pi \left( \frac{t}{P_i} + \phi_i \right)$$

where,  $P_i$  are the periods,  $a_i$  are the amplitudes for corresponding periods,  $mag_0$  is the base magnitude,  $\phi_i$  are the phases of periods. Once the baseline is simulated, the dips can be modelled in three steps: a fading part, the dip  $m(t) = m_b(t) + A$  where  $A$  is the amplitude of the dip, and a slow recovery phase (the approximate recovery time is 100 days).

## 5.6 Eclipsing binaries

Eclipsing binaries, while being variables, are treated as binaries and the eclipses are computed from the orbits of the components. See section 4.

## 5.7 Extragalactic variabilities

The variability of AGN and quasars is taken into account by light curves defined in the package LCmodel.jar produced by CU7. The parameters of the light curves have been checked to be consistent with the expectation.

## 5.8 Gamma ray Burst

GRBs are distributed uniformly over the entire sky. Based on the Swift satellite detections there is roughly 600 GRBs per year over the whole sky. However, only half of them exhibit optical afterglows, giving a rate of 300 afterglows per year. Current description of the afterglows light curve model is based on study done by Andreja Gomboc (Ljubljana), who compiled the data of GRBs from GRBs Coordinate Network Circulars (GCN). It is useful to define time  $t_1$  to 1 minute after the GRB trigger ( $t_0$ ) and, respectively,  $mag_1$  to magnitude at that time. Hence:

$$mag(t) = mag_1 + 0.5\alpha \log((t - t_0)/1min)$$

where  $\alpha$  between 0.4 and 1.4 and  $mag_1$  follows a Gaussian distribution with  $\sigma = 1.57$  and  $x_0 = 16.25$ .

## 6 Planetary nebulae

Planetary nebulae are generated using the Bruzual & Charlot isochrones for bulge population (solar metallicity, alpha enhanced, 10 Gyr) and for disc population (all ages, solar metallicity). This generates planetary nebulae from a luminosity function and corresponding effective temperature distribution in the same format as the Hess diagram used for ordinary stars. The spatial distribution follows the one of parent population. The type of the nebula is drawn at random among four types : Round (17%), elliptical (56%), bipolar (12%) and anomalous (15%). Spectra and shape are not yet attributed to these objects. It is planned to attribute a shape from a library of observed images of known nebula of each type, as is done for galaxies.

The library of PN images is based on images courteously provided by A. Manchado, of the Instituto de Astrofísica de Canarias, see <http://www.iac.es/nebu/nebula.html> In order to have an homogeneous sample, the images obtained with the Halph filter only have been selected. The images have then be processed according to the following procedure:

1. Rebinned if necessary so that all the images are 492x492 pixels
2. Removal of field stars, if any ( different procedures depending on the characteristics of the images)
3. For the images with a central star, two versions have been produced: one with the central star and one without
4. As we have no information on the PN absolute surface brightness, for each image, two attenuation factors have been applied: the first one decreases the brightness of the PN to 30% of its original value. The second one decreases it to 60% of its original value. Note that the brightness of the PN is decreased with respect to the

central star when it is there or with respect to the background sky if there is no central star

The final library of images therefore contains a bit more than 50 images, based on 18 original images. All PN types are present (Spherical, Elliptical, Bipolar and Various) but with a majority of spherical and elliptical ones.

These PN images can be linked directly to Gibis for generating images but not in other simulators.

## 7 Exoplanet simulation

Extra-solar planet simulation is described in Sozzetti (2007). To summarize, one or two extra-solar planets are generated with distributions in true mass  $M_p$  and orbital period  $P$  resembling those of Tabachnik & Tremaine (2002), which constitute quite a reasonable approximation to the observed distributions as of today, and extrapolated down to the masses close to the mass of Earth. Semi-major axes are derived given the host mass, planet mass, and period. Eccentricities are drawn from a power-law-type distribution, somewhat resembling phenomenologically diffusion processes in phase space. Full circularization ( $e = 0.0$ ) is assumed for periods below 6 days. All orbital angles ( $i$ ,  $\omega$ , and  $\Omega$ ) are drawn from uniform distributions. Observed correlations between different parameters (e.g.  $P$  and  $M_p$ ) are reproduced. Simple prescriptions for the radius (assuming a mass-radius relationship from available structural models, see e.g. Baraffe et al. (2003)), effective temperature, phase, and albedo (assuming toy models for the atmospheres, such as a Lambert sphere) are provided, based on the present-day observational evidence. The issue of how to smoothly bridge the generation of planets and stellar companions in the grey area corresponding to companion masses in the brown dwarf regime is left for future discussion.

For every dwarf star generated of spectral type between F and mid-K, the likelihood that it harbours a planet of given mass and period depends on its metal abundance according to the Fischer & Valenti (2005) and Sozzetti et al. (2009) prescriptions. M dwarfs, giant stars, white dwarfs, and young stars do not have planets for the time being, as well as double and multiple systems. The astrometric displacement, spectroscopic radial velocity amplitude, and photometric dimming (when transiting) induced by a planet on the parent star, and their evolution in time, are presently computed similarly to double and multiple stellar systems.

## 8 Extinction model

The extinction model used at present in the Gaia Simulator is described in Drimmel (2002). It is based on the dust distribution model of Drimmel (2002) with improvement with respect to

TABLE 8: Assumed parameters of the Magellanic clouds

Parameter	Unit	LMC	SMC	Reference
Distance	kpc	48.1	60.6	LMC: Macri et al. (2006) SMC: Hilditch et al. (2005)
Depth	kpc	0.75	1.48	LMC: Sakai et al. (2000) SMC: Subramanian & Subramaniam (2009)
$\mu_{\alpha \cos \delta}$	mas/yr	1.95	0.95	Costa et al. (2009)
$\mu_{\delta}$	mas/yr	0.43	-1.14	Costa et al. (2009)
$V_{los}$	km/s	283.	158.	SIMBAD (CDS)
Fe/H	dex	$-0.75 \pm 0.5$	$-1.2 \pm 0.2$	Kontizas et al, 2010, in prep
$\alpha/\text{Fe}$	dex	$0. \pm 0.2$	$0. \pm 0.2$	Kontizas et al, 2010, in prep

the correction based on FIR data and on spiral arm geometry. This full 3D extinction model is a strong improvements over previous generations of extinction models as it includes both a smooth diffuse absorption distribution for a disc and the spiral structure and smaller scale corrections based on the integrated dust emission measured from the FIR. Some uncertainties remain in the way the correction is applied, the choice of which component should be corrected not being trivial. In the future alternate models will be evaluated and tested to improve the quality of the simulations specially in the Galactic plane.

Since cycle 4, the interstellar extinction model is applied to Galactic and extragalactic objects.

Since cycle 10, small scale variations of the extinction are simulated by adding a dispersion on  $A_v$  on a star by star basis. This dispersion is 10% of the mean extinction at the distance of the star.

## 9 Extragalactic objects

### 9.1 Resolved galaxies

In cycle 8 we have implemented simulations of the Magellanic clouds in the following way. Catalogues of stars known to be part of both clouds (LMC and SMC) and their characteristics (magnitudes B, V, I, Teff,logg, spectral type) have been obtained from the literature (Belcheva et al., private communication). For the astrometry, since star by star information is missing, we assume a single proper motion and radial velocity for all stars of both clouds. Chemical abundances are also guessed from the mean abundance taken from the literature. The resulting values and their references are given in table 6. For simulating the depth of the clouds we assume a gaussian distribution along the line of sight with a sigma given in the table.

Stellar masses are estimated for each star from polynomial fits of the mass as a function of B-V colour, for several ranges of  $\log(g)$ . It is based on Padova isochrones for a metallicity of  $z=0.003$  for the LMC and  $z=0.0013$  for the SMC. The gravities have been estimated from the effective temperature and luminosity class but is very difficult to assert from the available observable. Hence the resulting HR diagrams for the Magellanic clouds are not as well defined and reliable as they would from theoretical isochrones.

Binaries and multiple stars are generated, as in the Milky Way, including eclipses. Other stellar variabilities are not included. There are no plan to include extended objects like nebulae in the Magellanic clouds.

No other resolved galaxy simulations are planned, unless explicit requests and corresponding manpower exist.

## 9.2 Unresolved galaxies

Unresolved galaxies are generated using the Stuff (catalogue generation) and Skymaker (shape/image simulation) codes from E. Bertin, adapted to Gaia by C. Dollet. These are C program called from the Java code. They have been translated into Java by A. Martins for Stuff and C. DelleLucche for Skymaker. The galaxy simulator generates a mock catalog of galaxies with a 2D uniform distribution and a distribution in each Hubble type sampled from Schechter's luminosity function (Fioc & Rocca-Volmerange (1999a); Schechter (1976)). Each galaxy is assembled as a sum of a disc and a spheroid. Each galaxy is put at its redshift and luminosity and K corrections are applied. The algorithm returns for each galaxy its position, magnitude, B/T relation, disk size, bulge size, bulge flatness, redshift, position angles, and V-I.

A library of low resolution spectra has been done based on Pegase-2 code ([www.iap.fr/pegase](http://www.iap.fr/pegase)). Details of the creation fo this library can be found in Livanou et al. (2009). 9 Hubble types are now available, with 5 different inclinations (0.00, 22.5, 45.0, 67.5, 90.0) for non-elliptical galaxies, and at 11 redshifts (from 0. to 2. by step of 0.2). For all inclinations, PEGASE.2 spectra are computed with internal extinction by transfer model with two geometries either slab or spheroid depending on type. Parameters of the luminosity function for each Hubble type are given in table 7.

A shape image can be associated to the galaxy through the Magil package. Currently Magil associates to the galaxy a shape taken from the Frei catalog according to the galaxy surface brightness, type (S, E, I), axis ratio and major axis.

## 9.3 Quasars

QSOs are simulated from the scheme proposed in Slezak & Mignard (2007). To summarize, lists of sources have been generated with similar statistical properties as the SDSS, but extrap-

TABLE 9: Parameters defining the luminosity function for different galaxy types at  $z=0$ , from Fioc & Rocca-Volmerange (1999b). The LF is from Schechter (1976). Parameters are :  $\Phi^*$ ,  $M^*$  and  $\alpha$ . 5th column gives the bulge to total ratio.

Type	$\Phi^*$ $\text{Mpc}^{-3}$	$M^*$ mag	$\alpha$	Bulge/Total
E2	1.91e-3	-20.02	-1.	1.0
E-SO	1.91e-3	-20.02	-1.	0.9
Sa	2.18e-3	-19.62	-1.	0.57
Sb	2.18e-3	-19.62	-1.	0.32
Sbc	2.18e-3	-19.62	-1.	0.32
Sc	4.82e-3	-18.86	-1.	0.016
Sd	9.65e-3	-18.86	-1.	0.049
Im	9.65e-3	-18.86	-1.	0.
QSFG	1.03e-2	-16.99	-1.73	0.

olated to  $G = 20.5$  (the SDSS sample being complete to  $i = 19.1$ ) and taking into account the flatter slope expected at the faint-end of the QSO luminosity distribution. The space density per bin of magnitude and the luminosity function should be very close to the actual sky distribution. Since bright quasars are saturated in the SDSS, the catalogue is complemented by the Véron-Cetty & Véron (2006) catalogue of nearby QSOs.

The equatorial coordinates have been generated from a uniform drawing on the sphere in each of the sub-populations defined by its redshift. No screening has been applied in the vicinity of the Galactic plane since this will result directly from the application of the absorption and reddening model at a later stage, when the catalogue is used to generate the observations. Distance indicators can be derived for each object from its redshift value by specifying a cosmological model. Each of these sources lying at cosmological distances, a zero parallax has been assigned to all of them. However to avoid possible overflow/underflow problems with a true zero parallax we have actually set all the parallax to  $10^{-6}$  mas, equivalent to an Euclidean distance of about 1 Gpc.

In principle distant sources are assumed to be co-moving with the general expansion of the distant Universe and have no transverse motion. However the observer is not at rest with respect to the distant Universe and the accelerated motion around the Galactic center, or more generally that of the Local group toward the Virgo cluster is the source of a spurious proper motion with a systematic pattern. This has been discussed in many places (Kovalevsky 2003; Mignard 2005). Eventually the effect of the acceleration (centripetal acceleration of the solar system) will show up as a small proper motion of the quasars, or stated differently we will see the motion of the quasars on a tiny fraction of it aberration ellipse whose period is 250 million years. This effect is simulated directly in the quasar catalogue, and equations given in Slezak & Mignard (2007). This explains their not null proper motions in the output catalogue.



TABLE 10: Probability of having a SN of type I or II for each Hubble type.

Hubble type	SNII Probability	SNI Probability
E2	0.	0.05
E-S0	0.	0.05
Sa	0.4	0.11
Sb	0.62	0.13
Sbc	1.07	0.16
Sc	0.16	0.07
Sd	0.049	0.07
Im	0.60	0.05
QSFG	0.	0.05

The new QSO catalogue includes about 2 million quasars but only about 100 000 of them are brighter than  $G=20$ . A subset is used for ordinary simulations with QSO brighter than 20.5. It contains 157230 QSOs. For each of them the slope of the spectrum and the equivalent width is available in order to compute the corresponding spectrum. For the moment the spectrum is searched in the QSO spectral library and only the closest spectrum is taken into account (no interpolation between library spectra).

The catalogue of QSO is organized such that QSO are extracted from the catalogue on demand from an indexed table and not kept in memory.

From cycle 9 on, variability of AGN and QSOs is simulated using irregular light curves, from the LCmodel.jar package produced by CU7.

## 9.4 Supernovae

Supernova (SN) events are generated in two ways. A set of SN are generated associated with galaxies, with a proportion for each Hubble type, as given in table 9.4. In this case, the SN is situated at a distance randomly selected at less than a disc radius from the parent galaxy, accounting for the inclination.

Another set of SN are generated randomly on the sky to simulate SN on host galaxies which are too faint in surface brightness to be detected by Gaia.

Four SN types are available with a total probability of occurring determined to give at the end 6366 SN per steradian during the 5 year mission (from estimations by Belokurov & Evans (2003)). For each SN type a probability is associated as well as an expected absolute magnitude with a dispersion. These parameters are given in table 8. Supernova like curves are from Peter Nugent ([http://supernova.lbl.gov/nugent/nugent\\_templates.html](http://supernova.lbl.gov/nugent/nugent_templates.html)). We first assume that the SN



TABLE 11: Parameters for each supernova type.

Type	Probability	$M_G$	Sigma
Ia	0.6663	-18.99	0.76
Ib/c	0.0999	-17.75	1.29
II-L	0.1978	-17.63	0.88
II-P	0.0387	-16.44	1.23

varies the same way at each wavelength (variable spectra will be considered later). In the mean time we have taken as reference the light curve in V.

## 10 Backgrounds

Backgrounds will play a significant role in the reduction process, perturbing the detection of objects and biasing their measurements. Two types of backgrounds are presently available : a constant background and a variable background image. For the constant background a solar spectrum is associated by default. For the variable background, the image must be provided by the user (no database yet other than the GIBIS one) and must contain either an HST FITS header or the following keywords : EXPTIME, MAGZERO, CDELTA1/CDELTA2. The image band is assumed to be the V band and a solar spectra is applied by default. Note that for experiment, the universe model can deal with some spectra of nebula (provided by G. Stasinska) and with the Orion nebula spectra and can deal with the HST F656N filter instead of the V band. This functionality can be added for future cycles on request and extended to other spectra and filters.

## 11 Radiation environment

The radiation environment will have effects on the CCD aging. The instrument model (DU4) will simulate the damage caused by the radiation environment. However a model for the expected radiation environment of the satellite during the mission has still to be provided. This task will be conducted by the Gaia Prime Contractor and the Space Environment Section at ESTEC. An interface between the project team and the simulation team ensures that Galactic cosmic ray and solar particle fluxes and spectra adopted by simulations are consistent with best knowledge at any given time.

## 12 Spectral libraries

The spectral libraries that are presently available are:

1. the Basel2 library, at LR (low resolution), that is used for BP and RP data simulations of normal stars,
2. the Marcs, the A-stars, the OB-stars and the WD-stars libraries. There is a LR and a HR (high resolution) version. These libraries are used for BP/RP and RVS simulations of normal stars.
3. the Phoenix library has a LR and a HR version, and can be used for BP/RP and RVS simulations of normal stars.
4. the Kurucz library, at HR can be used for RVS simulations of normal stars.
5. the Balmer emission lines libraries (Be). There is a LR version used for BP/RP simulations and a HR version used for RVS simulations of Be stars.
6. the QSO library, at LR, used for BP/RP QSOs simulations.
7. the Galaxy library at LR, used for BP/RP Galaxies simulation but can also be used for RVS background galaxies simulations

All the LR libraries are also used for photometric computations. The Marcs, the A, OB, WD stars, the Kurucz, the Be and the QSO libraries have been explicitly calculated for Gaia Simulation purposes, and they are calculated in vacuum. The Basel2 library is instead calculated using the air refractive index.

The Basel2 star library contains 8286 spectra covering the wavelength range 9.1 to 16000 nm with a mean resolution of 1 nm in the UV and of 2 nm in the visible. The ranges of fundamental parameters are: effective temperature  $T_{\text{eff}}$ : between 2000 and 50000 K, logarithmic surface gravity  $\log g$  between  $\sim -1$  and 5.5, and  $[\text{Fe}/\text{H}]$ : between +1.0 and -5.0. The spectra are not normalized to the continuum and are expressed in  $\text{erg/s/cm}^2/\text{hz}$ . The files are in ASCII format, they are stored in sub-folders depending on the metallicity value. The sub-folder name represents the  $[\text{Fe}/\text{H}]$  value: (e.g. M01 for  $[\text{Fe}/\text{H}]=-0.1$ , P10 for  $[\text{Fe}/\text{H}]=+1$ ). The spectra filename contains the informations on the star parameters (e.g. T07250GP400M10VT200XH125.dat for  $T_{\text{eff}} = 7250\text{K}$ ,  $\log g=+4$ ,  $[\text{Fe}/\text{H}]=-1$ . The VT microturbulent velocity and the XH mixing length parameter are fixed for all spectra). See [http://www.mpia.de/GAIA/icap/photosim/basel2.2\\_readme](http://www.mpia.de/GAIA/icap/photosim/basel2.2_readme) for a detailed description of the library.

The Marcs library has been provided by the CU8. The original library "StarNormal03" together with its readme file, is available from the CNES web site:

<http://internet1-ci.cnes.fr:8010/sourceLib.html>. The effective temperatures range between 4000 and 8000K (step 250K), the logarithmic surface gravities between -1.0 to 5.0 (step 0.5), and the overall metallicities between -5.0 and 1.0 (with a variable step from 1.0 to 0.25 dex). The fluxes are expressed in  $\text{W/m}^2/\text{nm}$ . From the original files we have separated the LR and the HR libraries. The LR library is only dependent on the fundamental atmospheric parameters  $T_{\text{eff}}$ ,

$\log g$  and  $[\text{Fe}/\text{H}]$  and contains 1778 spectra. All the original spectra have been kept. The HR library, instead, depends also on  $\alpha$ -elements (values -0.2, 0, 0.2, 0.4). The original HR library also depends on abundances in O, Mg, Si, etc. but these dependencies are not operational in this version. We have selected from the original library the first spectra with a given  $T_{\text{eff}}$ ,  $\log g$  and  $[\text{Fe}/\text{H}]$  and  $\alpha$ . The number of selected spectra is 7168. For each metallicity there are 2 files, one containing the parameters and the other the spectra. The file name contains information on the metallicity ( $[\text{Fe}/\text{H}]$ ) and on the resolution (LR/HR); i.e. "Marcsm150LR.params" is the file containing the parameters of the spectra LR with  $[\text{Fe}/\text{H}] = -1.5$ . The .params file contains as a first line the total number of spectra contained in the file. The following 4 columns: 1) serial number of the spectrum 2)  $T_{\text{eff}}$ , 3)  $\log g$ , and 4)  $\alpha$  elements abundance. The  $[\text{Fe}/\text{H}]$  is given directly in the file name. The spectrum corresponding to each .param file line is in the .spectra file at line+1 (spectra has not the first line containing the total number).

The Phoenix library has been provided by the CU8 (R.Sordo), but it is not available from the CNES web site and no readme file is available. The effective temperatures range between 3000 and 10000K, with steps of 100K from 3000K to 7000K and of 200K from 7000K to 10000K. The steps in  $\log g$  are of 0.5 and the grid start at different values depending to  $T_{\text{eff}}$ : at -0.5 (between 3000K and 5700K), at 0 (between 5800K and 6200K), at 0.5 (between 6300K and 7000K), at 1 (between 7200K to 8800K) and at 1.5 (from 9000K to 10000K). The  $\log g$  grid ends at 5.5 for all temperatures. The  $[\text{Fe}/\text{H}]$  ranges from -2.5 to +0.5 with steps of 0.5. Both LR and HR libraries are only dependent on the fundamental atmospheric parameters  $T_{\text{eff}}$ ,  $\log g$  and  $[\text{Fe}/\text{H}]$ . The  $\alpha$ -elements are set to 0. The LR library contains 4575 spectra and the HR 4561 (the spectra with  $T_{\text{eff}}=3000$  and  $[\text{Fe}/\text{H}]=0$  are missing).

The OB, the A and the WD stars libraries have been provided by the CU8. The original libraries called respectively StarNormal01, StarNormal02 and StarNormal05 with their readme files are available from the CNES web site. From the original files we have separated the LR and HR libraries. The OB and the WD libraries are only dependent on the atmospheric parameters  $T_{\text{eff}}$ ,  $\log g$ ;  $[\text{Fe}/\text{H}]$  is fixed to the solar value for all spectra. The number of spectra in both the LR and the HR libraries is 213 (OB) and 129 (WD). The A library instead contains also the  $[\text{Fe}/\text{H}]$  dependence and the number of spectra is 972 in both the LR and the HR libraries. The .params files contain as a first line the total number of spectra contained in the file. The following 3 columns are: 1)  $T_{\text{eff}}$ , 2)  $\log g$  and 3)  $[\text{Fe}/\text{H}]$ . As for all the fluxes provided by the CU8 the units are  $\text{W}/\text{m}^2/\text{nm}$  (Thevenin (2008)), and the wavelength range is 300, 1100 nm for LR and 840, 890 nm for LR.

The Kurucz library has high resolution,  $R=250\,000$ , and spectral range between 840-880 nm. It contains 33 star spectra produced using the Kurucz model (Kurucz R., 1993, SYNTHE Spectrum Synthesis Program and Line data. S.A.O., Cambridge, MA, CD-ROM No.18) using the ATLAS 9 models of F. Castelli (<http://wwwuser.oats.inaf.it/castelli/grids.html>) computed with the new opacity distribution (Sbordone et al. 2004). We used a grid of  $T_{\text{eff}}$  between 4000 and 40 000K (not uniform steps),  $\log g$  of 2.5, 4 and 4.5, and solar metallicity ( $[\text{Fe}/\text{H}]=0$ ). The spectra are not normalized to the continuum and are expressed in  $\text{erg}/\text{s}/\text{cm}^2/\text{Hz}$ . The files are

in ASCII format and the filename contains the informations on the star physical parameters (e.g. ap00t5500g40k2odfnew\_w840\_880.asc : p00 indicates  $[\text{Fe}/\text{H}]=0$ , t5500 the effective temperature ( $T_{\text{eff}}=5500$  K), g40 logarithmic surface gravity ( $\log g=4.00$ ), the microturbulent velocity and the mixing length are fixed to 2 km/s for all spectra). The flux values are given in  $\text{erg/s/cm}^2/\text{hz}$  (in the second column of the files), the wavelengths in Å (in the first column of the files) In the third column the flux in the continuum is given and in the fourth the flux normalized to the continuum.

The Be stars library have been calculated by Yves Fremat. In these version there are 174 LR spectra and 174 HR spectra. The fluxes are expressed in  $\text{W/m}^2/\text{nm}$ . The  $T_{\text{eff}}$  are of 15000 K, 20000 K and 25000 K;  $\log g=4$  and  $[\text{Fe}/\text{H}] = 0$ . The parameter used to indicate the strength of the emission features is the ratio between the envelope radius and the stellar radius ( $R_{\text{env}}/R_{\text{star}}$ ). There are 174 LR and 174 HR spectra separated in 2 files called FrematBeLR.spectra and FrematBeHR.spectra, the relative parameters are contained in the FrematBe.param. This library is also described and available via the CU8 wiki page : CU8-:Spectral\_Libraries:-general.

The QSO library have been calculated by Jean-Christophe Mauduit at LR and contains 2000 spectra. The parameters used are  $z$ ,  $W$  (equivalent width) and the *Slope*. The files are in ASCII format and the filename contains the informations on the parameters: (e.g. 1.62\_ - 0.2\_1363.dat indicates that  $z = 1.62$ ,  $Slope=-0.2$ ,  $W=1363$ ). The wavelengths are given in Å in the first column of the file and the fluxes are given in relative values in  $\text{erg/s/cm}^2/\text{Å}$  in the second column of the file. The spectra are calculated in a random grid of parameters.

The Galaxy library has been created from PEGASE.2 ([www.iap.fr/pegase](http://www.iap.fr/pegase)) and described in Livanou et al. (2009). The parameters used are  $z$  with range  $[0, 0.2]$ , steps 0.02; Spectral type: there 9 types numbered from 1 to 9 corresponding to the Hubble types E2, E\_SO, Sa, Sb, Sbc, Sc, Sd, Im, and QSFG (quenched star forming galaxy; Inclination with range  $[0,90]$  degrees, and steps of 22.5. The original file is called synthetic\_galaxies.dat. We have separated the parameters (for CPU time reasons) in the file synthetic\_galaxies.params containing 1)  $z$ , 2) spectral type, 3) inclination and 4) bolometric magnitude (not used in spectra selection).

The association of a spectrum to an AstroSource is done based on a minimum distance method between the PhysicalParameters of the source and those of the spectrum. For normal stars the parameters used in general are:  $T_{\text{eff}}$ ,  $\log g$  and  $[\text{Fe}/\text{H}]$ , but for Marcs HR library also the  $\alpha$ -elements are used. A linear interpolation in these parameters can be done for the LR normal stars libraries. In the case of RVS simulations, if the StellarSource has  $v_{\text{ini}} > 5\text{km/s}$ , a convolution with a rotational profile is done. For Be stars the parameter  $R_{\text{env}}/R_{\text{star}}$  is also used. When a star is classified as Be a spectrum is selected from this library, but since the range in the atmospheric parameters  $T_{\text{eff}}$  and  $\log g$  of the Be library is poor, it can happen that the spectral parameters are not close to the source ones.

The number of spectral libraries is expected to increase regularly in order to allow the spectroscopic simulation of all types of sources of the Universe model.

## 13 References

- Arenou F., january 2010, The simulated multiple stars, Tech. rep., Observatoire de Paris-Meudon, gAIA-C2-SP-OPM-FA-054
- Arenou F., Reyl  C., Babusiaux C., et al., 2008, Identification of simulated sources, Tech. Rep. GAIA-C2-SP-OPM-FA-049, Observatoire de Paris, URL <http://wwwhip.obspm.fr/~arenou/PS-papers/gaia/GAIA-C2-SP-OPM-FA-049.pdf>
- Baraffe I., Chabrier G., Barman T.S., Allard F., Hauschildt P.H., May 2003, A&A, 402, 701
- Belokurov V.A., Evans N.W., May 2003, MNRAS, 341, 569
- Bensby T., Alves-Brito A., Oey M.S., Yong D., Mel ndez J., Jun. 2010, A&A, 516, L13+
- Bienayme O., Robin A.C., Creze M., Jun. 1987a, A&A, 180, 94
- Bienayme O., Robin A.C., Creze M., Nov. 1987b, A&A, 186, 359
- Costa E., M ndez R.A., Pedreros M.H., et al., May 2009, AJ, 137, 4339
- Drimmel R., August 2002, Galactic absorption model: refined version, Tech. rep., gAIA\_SWG\_RD\_03
- Drimmel R., Bucciarelli B., Lattanzi M.G., Smart R., Spagna A., April 2003, All sky source counts to  $R_F = 20$  using GSC-II, Tech. rep., IOT, gAIA\_ML\_20
- Eyer L., Robin A., Evans D.W., Reyl  C., June 2005, Implementation of variable stars in the Galactic model. I. General concept, Tech. rep., OG, vSWG-LE-002
- Fioc M., Rocca-Volmerange B., Apr. 1999a, A&A, 344, 393
- Fioc M., Rocca-Volmerange B., Nov. 1999b, A&A, 351, 869
- Fischer D.A., Valenti J., Apr. 2005, ApJ, 622, 1102
- Gomez A.E., Grenier S., Udry S., et al., Aug. 1997, In: ESA Special Publication, vol. 402 of ESA Special Publication, 621–624
- Gonzalez O.A., Rejkuba M., Zoccali M., et al., Jun. 2011, A&A, 530, A54+
- Han C., Jul. 2008, ApJ, 681, 806
- Haywood M., Robin A.C., Creze M., Apr. 1997a, A&A, 320, 428

- Haywood M., Robin A.C., Creze M., Apr. 1997b, A&A, 320, 440
- Hilditch R.W., Howarth I.D., Harries T.J., Feb. 2005, MNRAS, 357, 304
- Jaschek C., Jaschek M., Egret D., Andrillat Y., Mar. 1988, A&A, 192, 285
- Kochukhov O., Jun. 2007, Communications in Asteroseismology, 150, 39
- Kontizas E., Dapergolas A., Morgan D.H., Kontizas M., Apr. 2001, A&A, 369, 932
- Kovalevsky J., Jun. 2003, A&A, 404, 743
- Kowalski A.F., Hawley S.L., Hilton E.J., et al., Aug. 2009, AJ, 138, 633
- Kurtz D.W., Sep. 1982, MNRAS, 200, 807
- Livanou E., Kontizas M., Karamelas A., et al., August 2009, Library of typical synthetic galaxy spectra for the Gaia Universe Model simulator, Tech. rep., UOA, gAIA-C8-TN-UOA-EL-001-1
- Macri L.M., Stanek K.Z., Bersier D., Greenhill L.J., Reid M.J., Dec. 2006, ApJ, 652, 1133
- Mignard F., Jan. 2005, In: Turon C., O’Flaherty K.S., Perryman M.A.C. (eds.) The Three-Dimensional Universe with Gaia, vol. 576 of ESA Special Publication, 5–+
- Reid I.N., Gizis J.E., Hawley S.L., Nov. 2002, AJ, 124, 2721
- Reylé C., Robin A., Arenou F., Grux E., July 2007, Universe Model Interface Control Document, Tech. rep., Obs. de Besançon, Obs. de Paris-Meudon, gAIA-C2-SP-LAOB-CR-001
- Reylé C., Marshall D.J., Robin A.C., Schultheis M., Mar. 2009, A&A, 495, 819
- Robin A.C., Reylé C., Derrière S., Picaud S., 2003, Astronomy & Astrophysics, 509, 523
- Sakai S., Zaritsky D., Kennicutt R.C. Jr., Mar. 2000, AJ, 119, 1197
- Sbordone L., Bonifacio P., Castelli F., Kurucz R.L., 2004, Memorie della Societa Astronomica Italiana Supplement, 5, 93
- Schechter P., Jan. 1976, ApJ, 203, 297
- Slezak E., Mignard F., August 2007, A realistic QSO Catalogue for the Gaia Universe Model, Tech. rep., OCA, gAIA-C2-TN-OCA-ES-001-1
- Soszyński I., Udalski A., Szymański M.K., et al., Dec. 2009, Acta Astronomica, 59, 335
- Sozzetti A., November 2007, Simulations of Planetary Systems in the Gaia Universe Model, Tech. rep., OATO, gAIA-C2-TN-OATO-ASO-001-2
- Sozzetti A., Torres G., Latham D.W., et al., May 2009, ApJ, 697, 544

Stift M.J., Alecian G., Apr. 2009, MNRAS, 394, 1503

Subramanian S., Subramaniam A., Mar. 2009, A&A, 496, 399

Tabachnik S., Tremaine S., Sep. 2002, MNRAS, 335, 151

Thevenin F., September 2008, ICD for the Gaia synthetic spectral libraries, Tech. rep., OCA, gAIA-C8-SP-OCA-SP-002

Twarog B.A., Nov. 1980, ApJ, 242, 242

van der Hucht K.A., Feb. 2001, New Astronomy Review, 45, 135

Véron-Cetty M.P., Véron P., Aug. 2006, A&A, 455, 773

Zorec J., Briot D., Feb. 1997, A&A, 318, 443